

The $^{12}\text{C}/^{13}\text{C}$ ratio in the Planetary Nebula NGC 3242 from *Hubble Space Telescope* STIS observations¹

Francesco Palla, Daniele Galli, Alessandro Marconi

INAF – Osservatorio Astrofisico di Arcetri
Largo Enrico Fermi 5
I-50125 Firenze, Italy

palla,galli,marconi@arcetri.astro.it

Letizia Stanghellini²

Space Telescope Science Institute
3700 San Martin Drive
Baltimore MD 21218, USA

lstanghe@stsci.edu

and

Monica Tosi

INAF – Osservatorio Astronomico di Bologna
Via Ranzani, 1
I-40127 Bologna, Italy

tosi@bo.astro.it

ABSTRACT

We present high resolution HST ultraviolet spectroscopy of NGC 3242, the only planetary nebula with a measured abundance of ^3He . The Space Telescope Imaging Spectrograph (STIS) has been used to observe the CIII multiplet near $\lambda 1908 \text{ \AA}$. The presence of ^{12}C and ^{13}C lines at these wavelengths allows a direct estimate of the carbon isotopic ratio in the ionized gas of the nebula. We have detected the ^{12}C doublet and obtained an upper limit on the ^{13}C $\lambda 1909.6 \text{ \AA}$ line, resulting in a carbon isotopic ratio

¹Based on observations with the NASA/ESA *Hubble Space Telescope*, obtained at the Space Telescope Science Institute, which is operated by the Association of Universities for Research in Astronomy (AURA), Inc., under NASA contract NAS 5–26555.

²Affiliated with the Astrophysics Division, Space Science Department of ESA; on leave from INAF–Osservatorio Astronomico di Bologna

$^{12}\text{C}/^{13}\text{C} > 38$, in agreement with standard stellar models. The lack of the ^{13}C line and the presence of the ^3He line in the spectrum indicate that the progenitor star did not undergo a phase of deep mixing during the last stages of its evolution. The significance of this result for studies of stellar nucleosynthesis and Galactic chemical evolution is discussed.

Subject headings: (ISM:) planetary nebulae: individual (NGC 3242) – ISM: abundances – stars: evolution – Galaxy: evolution

1. Introduction

In principle, the abundance of ^3He in our Galaxy can be used to test the predictions of Big-Bang nucleosynthesis and to provide constraints on the baryon density of the Universe (e.g. Bania et al. 2002). However, the usefulness of ^3He as a *cosmic baryometer* is limited by a poor understanding of its evolution in our Galaxy, one of the major unsolved mysteries in the field of cosmic abundances. The problem was first recognized by Rood et al. (1976) who noted the strong discrepancy between the theoretical yields of low-mass stars, $X(^3\text{He}) \sim 10^{-3}$ for a $1 M_{\odot}$ star (Iben 1965), and the measured abundances in HII regions, $X(^3\text{He}) \sim 10^{-5}$ (Balsler et al. 1999a). Despite the increase in the number and quality of observational constraints and in the accuracy of stellar evolutionary calculations over the past 25 years, the ^3He problem is still with us today (e.g. Tosi 2001).

An interesting solution to the puzzle of ^3He based on stellar physics has been suggested by various groups (Hogan 1995; Charbonnel 1995). Accordingly, a non-standard mixing mechanism acting during the RGB and/or AGB phases of stars of mass up to $\sim 2M_{\odot}$ can effectively suppress the production of ^3He . In this way, low-mass stars are not ^3He producers and may even become net ^3He destroyers, lessening the tension between the results of chemical evolution models and observations. If this mechanism is indeed at work in low-mass stars, an unavoidable consequence is that the ratio of $^{12}\text{C}/^{13}\text{C}$ in the ejecta of planetary nebulae (PNe) should be much *lower* than in the standard case. For a $1M_{\odot}$ star, the predicted ratio is ~ 5 against the standard value of 25–30 (Boothroyd & Sackmann 1999). Thus, it is very important to have an accurate measure of the carbon isotopic ratio in those PNe where a high ^3He abundance has been determined. Should these nebulae show a $^{12}\text{C}/^{13}\text{C}$ ratio close to 25–30, then no modifications to the standard scenario would be required. Otherwise, one has to invoke another selective process (circulation, diffusion etc.) that operates on ^{13}C but not on ^3He .

NGC 3242 is the only PN with a firm detection of the $^3\text{He}^+$ hyperfine line at 8.67 GHz. The initial discovery indicated a value of $^3\text{He}/\text{H} \simeq 10^{-3}$ by number (Rood et al. 1992). Subsequent observations confirmed the detection and refined the estimate of the abundance to lower values, $^3\text{He}/\text{H} = (2 - 5) \times 10^{-4}$ (Balsler et al. 1999b). In both cases, the resulting values of ^3He agree with the predictions of standard stellar nucleosynthesis models (Rood et al. 1976).

In an attempt to derive the $^{12}\text{C}/^{13}\text{C}$ ratio in PNe, we observed at millimeter wavelengths a sample of 28 objects, determining the CO isotopic ratio in 14 of them and obtaining robust upper limits in 6 other nebulae (Palla et al. 2000). Unfortunately, no CO emission was detected in NGC 3242, so that we could not draw any conclusion about the occurrence of mixing in this PN. Following Clegg et al. (1997), we decided to adopt the complementary approach of observing the C III] multiplet near 1908 Å, exploiting the unique spectroscopic capabilities of HST/STIS at ultraviolet wavelengths. Clegg et al. (1997) measured for the first time the carbon isotopic ratio in the ionized gas of NGC 3918 and SMC N2, using the GHRS aboard the HST. The big advantage of this method over observations in the millimeter band is that the simultaneous presence of the ^{12}C and ^{13}C lines in this spectral region allows a *direct* estimate of the carbon isotopic ratio without having to worry about problems such as isotopic fractionation and optical depth effects that make the derivation of abundances from CO lines more uncertain (Sahai et al. 1994; Schöier & Olofsson 2000).

2. Observations and Results

NGC 3242 is a multiple-shell, attached halo PN, located at a distance of about 1 kpc (Stanghellini & Pasquali 1995). The inner and outer shells have diameters of 15'' and 29'', respectively. The inner shell (or rim) is characterized by the presence of two prominent spots in O I, O III, and N II. The post-AGB mass of the central star is estimated to be $M_{\text{CS}} = (0.56 \pm 0.01) M_{\odot}$, corresponding to a main-sequence mass of $M_{\text{MS}} = (1.2 \pm 0.2) M_{\odot}$ (Galli et al. 1997). The metallicity of NGC 3242 is $Z \simeq Z_{\odot}/2$ (Barker 1985).

We present high quality STIS observations of ^{12}C and ^{13}C in the ionized gas of NGC 3242 by using the C III] multiplet near 1908 Å. The multiplet has two lines, $^3\text{P}_1^0-^1\text{S}_0$ at 1908.7 Å and $^3\text{P}_2^0-^1\text{S}_0$ at 1906.7 Å which are intercombination and magnetic quadrupole transitions, and a third line, $^3_{1/2}\text{P}_0^0-^1_{1/2}\text{S}_0$ at 1909.6 Å, which is generally completely forbidden except in the case of the ^{13}C atom as a result of the non zero nuclear spin. The first two lines have different transition probabilities and their ratio has been used to determine the electron density in PNe and other low-density objects. The third line is weaker than the others (typically, less than one percent), and originates only in ^{13}C .

We observed NGC 3242 with STIS on the *HST* over 5 orbits in March 2001 for a total of 13000 seconds of integration time. All of the spectra were obtained through a $52'' \times 0''.1$ slit to maximize throughput without a significant loss in spectral resolution. The slit was positioned to cut through the two conspicuous spots of the rim, avoiding the central star. We used the MAMA detectors and G230M gratings whose range well encompasses the spectral region of interest, and whose pixel scale (0.09 Å per pixel) is adequate for our observations. The prime tilt was centered at 1933 Å, achieving a spectral resolution of 0.36 Å ($\sim 25 \text{ km s}^{-1}$) which is enough to resolve the C III] line at 1909.6 Å from the stronger C III] line at 1908.7 Å.

The spectra were recalibrated using the STIS pipeline and the best reference files available in the archive as of November 2001. The individual spectra from each orbit were independently calibrated in wavelength and flux, and resampled to a linear wavelength scale (retaining the same average dispersion). Careful examination of the spectra from each orbit reveals no discernible change in flux over time or as a function of position on the detectors. We therefore averaged the spectra (weighted by exposure time) to obtain the final versions of the G230M spectra. The spectrum was then obtained by coadding ~ 250 rows selected from the highest surface brightness regions coinciding with the two bright spots of the rim.

The resultant spectrum and its residuals are shown in Figure 1. The ^{12}C lines at 1906.7 Å and 1908.7 Å have fluxes of $(5.36 \pm 0.04) \times 10^{-13}$ and $(3.91 \pm 0.04) \times 10^{-13}$ erg cm $^{-2}$ s $^{-1}$ arcsec $^{-2}$, respectively, yielding a ratio of 1.37 ± 0.02 . For the ^{13}C line at 1909.6 Å, we have obtained a 1σ upper limit of $\sim 1.5 \times 10^{-15}$ erg cm $^{-2}$ s $^{-1}$ arcsec $^{-2}$. Thus, C III] 1909.6/1906.7 $< 2.8 \times 10^{-3}$.

The ^{12}C lines cannot be described with gaussian profiles because they present faint blue and red wings. As shown in Table 1, we fit the ^{12}C lines with two gaussian components with the same central wavelength but different fluxes and line widths. The bright narrow component has a FWHM of 52 km s $^{-1}$, significantly larger than the instrumental resolution of the G230M grating (~ 30 km s $^{-1}$); the broadening is probably due to the presence of two unresolved components coming from the receding and approaching edges of the nebula. The faint wings can be described with a gaussian profile with 290 km s $^{-1}$ FWHM, indicating the presence of fast moving gas.

Following Clegg et al. (1997), the 1906.7/1908.7 intensity ratio yields the electron density, while the 1909.6/1908.7 line ratio is used to determine the $^{12}\text{C}/^{13}\text{C}$ abundance ratio (see their Fig. 2). For a value of 1906.7/1908.7 = 1.4, we obtain an electron density $n_e = 8.9 \times 10^3$ cm $^{-3}$. This value is larger than that reported by Stanghellini & Kaler (1989) from a variety of forbidden lines of lower ionization ($n_e = 2.7 \times 10^3$ cm $^{-3}$), but still below the threshold for collisional quenching of the ^{13}C line ($n_e \simeq 2 \times 10^4$ cm $^{-3}$). Then, the expected 1909.6/1908.7 ratio computed assuming equal abundances of ^{12}C and ^{13}C is 0.15. Using the observed limit on 1909.6/1906.7 $< 2.8 \times 10^{-3}$, we infer a lower limit to the carbon isotopic ratio of $^{12}\text{C}/^{13}\text{C} > 0.15/(1.4 \times 2.8 \times 10^{-3}) \simeq 38$.

In Figure 2, we compare the observed $^3\text{He}/\text{H}$ (Balser et al. 1999b) and $^{12}\text{C}/^{13}\text{C}$ ratio (this work) of NGC 3242 with the predictions of standard and non standard models for the advanced phases of the evolution of stars in the mass range 1 to 3 M_\odot . Note that the largest discrepancy between the models occurs below $\sim 2M_\odot$, i.e for stars that do experience the helium flash. It is evident that standard models (left panels) reproduce very well the results in both cases, whereas the inclusion of extra-mixing processes fails by factors between 3 and 5. As noted above, the metallicity of NGC 3242 is lower than solar by about a factor of 2. For standard models, the ^3He yields are rather insensitive to Z , as shown by the calculations of Dearborn et al. (1996) (see their Fig. 1). Similarly, a 50% decrease of Z produces only a $\sim 20\%$ increase of the $^{12}\text{C}/^{13}\text{C}$ ratio (e.g. van den Hoek & Groenewegen 1997).

Considering the sensitivity of the non-standard models to metallicity, the effect is shown in

Fig. 2 where we plot two curves for $Z = 0.02$ and $Z = 0.007$. At lower metallicities, the depth of the convective zone is larger, implying higher temperatures and more efficient nuclear burning at the base of the convection region. Therefore, the predicted ${}^3\text{He}$ abundance *and* ${}^{12}\text{C}/{}^{13}\text{C}$ ratio are lower than in the solar case, and the discrepancy with the observed values becomes even larger.

3. Discussion

The HST observations reported here provide an independent support to the ${}^3\text{He}$ observations at 9.8 GHz and allow to draw firm conclusions about the nucleosynthesis history of NGC 3242. The lack of the ${}^{13}\text{C}$ line and the presence of the ${}^3\text{He}$ line in the spectrum indicate that the progenitor star did not undergo a phase of deep mixing during the late stages of its evolution. At first glance, this result may suggest that there is no need to revise standard nucleosynthesis models, since Fig. 2 shows that there is excellent agreement between their predictions and the values derived from the observations of both ${}^3\text{He}$ and ${}^{12}\text{C}/{}^{13}\text{C}$. However, the question is whether NGC 3242 is a special case among PNe.

The existence of isotopic anomalies in low-mass stars (below $\sim 3M_{\odot}$) is well documented for red giant stars (e.g. Charbonnel et al. 1998; Gratton et al. 2000). From the analysis of a large sample of field and cluster RGB stars, Charbonnel & do Nascimento (1998) conclude that more than 90% of them present ${}^{12}\text{C}/{}^{13}\text{C}$ ratios inconsistent with the results of standard models. The case for AGB stars is more controversial. Evidence for mixing comes from data on oxygen and carbon isotopic ratios (Wasserburg et al. 1995) and on ${}^7\text{Li}$ abundances (Charbonnel & Balachandran 2000), but its statistical significance is hard to assess. For example, J-type carbon stars clearly show ${}^{12}\text{C}/{}^{13}\text{C}$ ratios smaller than 10, well below the theoretical predictions (e.g. Abia & Isern 1997; Ohnaka & Tsuji 1999). Their progenitors appear to be low-mass stars with $M \lesssim 2 - 3M_{\odot}$, suggesting the operation of mixing processes (Abia & Isern 2000). However, J-type represent only $\sim 15\%$ of the whole C-star population. The occurrence of mixing in this class of stars finds support from the analysis of *s*-process elements in a sample of C(N)-type stars (Abia et al. 2001). These stars account for the majority of the C-stars and have values of ${}^{12}\text{C}/{}^{13}\text{C}$ greater than 10 but less than the solar value (89), consistent with model results only for $M \lesssim 1.5M_{\odot}$ (cf. Fig. 2). For $M \gtrsim 1.5M_{\odot}$, standard models predict a sharp rise of the ${}^{12}\text{C}/{}^{13}\text{C}$ ratio (up to ~ 100), which is quite sensitive to metallicity effects. The reduction of this ratio induced by the occurrence of deep mixing in the AGB phase cannot be quantified at present, and detailed modelling is obviously needed to clarify the situation.

Owing to the lack of non standard AGB yields, we show in the bottom right panel of Fig. 2 the results for RGB deep mixing. How representative are these numbers for the more advanced phases? From our previous estimate of the ${}^{12}\text{C}/{}^{13}\text{C}$ ratio in 20 PNe from CO line emission, we have found that the majority of them have ${}^{12}\text{C}/{}^{13}\text{C}$ ratios between 10 and 25 for masses 1.5 to $3 M_{\odot}$. These values are lower than those expected from standard AGB models, even in the case where the ${}^{12}\text{C}/{}^{13}\text{C}$ value was very low (~ 10) at the base of the AGB, as a result of deep mixing

during the RGB. The strong ^{12}C production by third dredge-up along the AGB raises the isotopic ratio to much higher values (Abia et al. 2001). Therefore, the overall evidence seems to indicate that active mixing occurs also in the early AGB phase. Returning to the case of NGC 3242, we may conclude that it must belong to the small group of “standard” low-mass stars, consisting of $\sim 10\%$ of stars with $M \lesssim 2 M_{\odot}$.

This point is of direct relevance to the ^3He problem in the context of Galactic chemical evolution. A very small percentage of low-mass stars producing large quantities of ^3He is required to explain the ^3He abundances measured in the pre-solar nebula, in the local ISM, and in HII regions (Palla et al. 2000). All these objects show $^3\text{He}/\text{H}$ ratios around 10^{-5} , lower than that measured in NGC 3242 by at least an order of magnitude.

The upper panel of Figure 3 shows the predictions of chemical evolution models assuming standard and non standard stellar nucleosynthesis and the most recent abundances measured in the solar system and local ISM. The model computed with the extra-mixing prescriptions of Sackmann & Boothroyd (1999) for 90% of low-mass stars fits very well the observations, whereas the standard model is systematically higher.

The failure of standard models is more dramatic when considering the Galactic radial distribution of ^3He , as shown in the bottom panel of Fig. 3. The mixing hypothesis improves significantly the agreement, and provides an upper envelope to the distribution of *simple* HII regions, i.e. those which are well described by homogeneous spheres (Bania et al. 2002). Bania et al. have argued that only these objects provide sufficiently accurate $^3\text{He}/\text{H}$ estimates for comparison with Galactic evolution models. Since *simple* HII regions have ^3He abundances systematically lower than the average, the implication is that almost 100% of low-mass stars should undergo non-standard nucleosynthesis. In that event, NGC 3242 would stand as a unique object in the Galaxy.

The research of D.G., F.P. and M.T. has been supported by grants COFIN 1998-MURST and COFIN 2000-MURST at the Osservatorio Astrofisico di Arcetri and Osservatorio Astronomico di Bologna.

REFERENCES

- Abia, C., & Isern, J. 1997, MNRAS, 289, L111
- Abia, C., & Isern, J. 2000, ApJ, 536, 438
- Abia, C., Busso, M., Gallino, R., Domínguez, I., Straniero, O., & Isern, J. 2001, ApJ, 559, 1117
- Balser, D.S., Bania, T.M., Rood, R.T., & Wilson, T.L. 1999a, ApJ, 510, 759
- Balser, D.S., Rood, R.T., & Bania, T.M. 1999b, ApJ, 522, L73

- Bania, T.M., Rood, R.T., & Balser, D.S. 2002, *Nature*, 415, 54
- Barker, T. 1985, *ApJ*, 294, 193
- Boothroyd, A., & Sackmann, I.-J. 1999, *ApJ*, 510, 232
- Charbonnel, C. 1995, *ApJ*, 453, L41
- Charbonnel, C., & do Nascimento, J.D. Jr. 1998, *A&A*, 336, 915
- Charbonnel, C., & Balachandran, S. 2000, *A&A*, 359, 563
- Charbonnel, C., Brown, J.A., & Wallerstein, G. 1998, *A&A*, 332, 204
- Clegg, R. E. S., Storey, P. J., Walsh, J. R., & Neale, L. 1997, *MNRAS*, 284, 348
- Dearborn, D. S. P., Steigman, G., & Tosi, M. 1996, *ApJ*, 465, 887
- Galli, D., Stanghellini, L., Tosi, M., & Palla, F. 1997, *ApJ*, 477, 218
- Geiss, J., & Gloeckler, G. 1998, *Space Sci. Rev.*, 84, 239
- Gratton, R., Sneden, C., Carretta, E., & Bragaglia, A. 2000, *A&A*, 354, 169
- Hogan, C.J. 1995, *ApJ*, 441, L17
- Iben, I. 1965, *ApJ*, 142, 1447
- Marigo, P. 2001, *A&A*, 370, 194
- Ohnaka, K., & Tsuji, T. 1999, *A&A*, 345, 233
- Palla, F., Bachiller, R., Stanghellini, L., Tosi, M., & Galli, D. 2000, *A&A*, 355, 69
- Rood, R.T., Steigman, G., Tinsley, B.M. 1976, *ApJ*, 207, L57
- Rood, R.T., Bania, T.M., & Wilson, T.L. 1992, *Nature*, 355, 618
- Sackmann, I.-J., & Boothroyd A. I. 1999, *ApJ*, 510, 217
- Sahai, R., Wootten, A., Schwarz, H.E., & Wild, W. 1994, *ApJ*, 428, 237
- Schöier, F.L., & Olofsson, H. 2000, *A&A*, 368, 969
- Stanghellini, L., & Kaler, J.B. 1989, *ApJ*, 343, 811
- Stanghellini, L., & Pasquali, A. 1995, *ApJ*, 452, 286
- Tosi, M. 2001, in *Cosmic Evolution*, ed. E. Vangioni-Flam, R. Ferlet, & M. Lemoine (Singapore: World Scientific), 77

van den Hoeck, L.B., & Groenewegen, M.A.T. 1997, A&A, 123, 305

Wasserburg, G.J., Boothroyd, A.I., & Sackmann, I.-J. 1995, ApJ, 447, L37

Weiss, A., Wagenhuber, J., & Denissenkov, P. A. 1996, A&A, 313, 581

Table 1. LINE PARAMETERS OF THE C III] MULTIPLET

Line	λ^a	Flux ^b	FWHM ^c
$^{12}\text{C } J = 2 \rightarrow 0$	1906.760 ± 0.001	4.85 ± 0.03	52.3 ± 0.2
	1906.760	0.51 ± 0.03	290 ± 25
$^{12}\text{C } J = 1 \rightarrow 0$	1908.81	3.50 ± 0.02	52.3
	1908.81	0.41 ± 0.03	290
$^{13}\text{C } F = \frac{1}{2} \rightarrow \frac{1}{2}$	1909.67	< 0.015	

^a Observed Wavelength (\AA).

^b Surface brightness ($10^{-13} \text{ erg cm}^{-2} \text{ s}^{-1} \text{ arcsec}^{-2}$).

^c Full Width at Half Maximum (km s^{-1}).

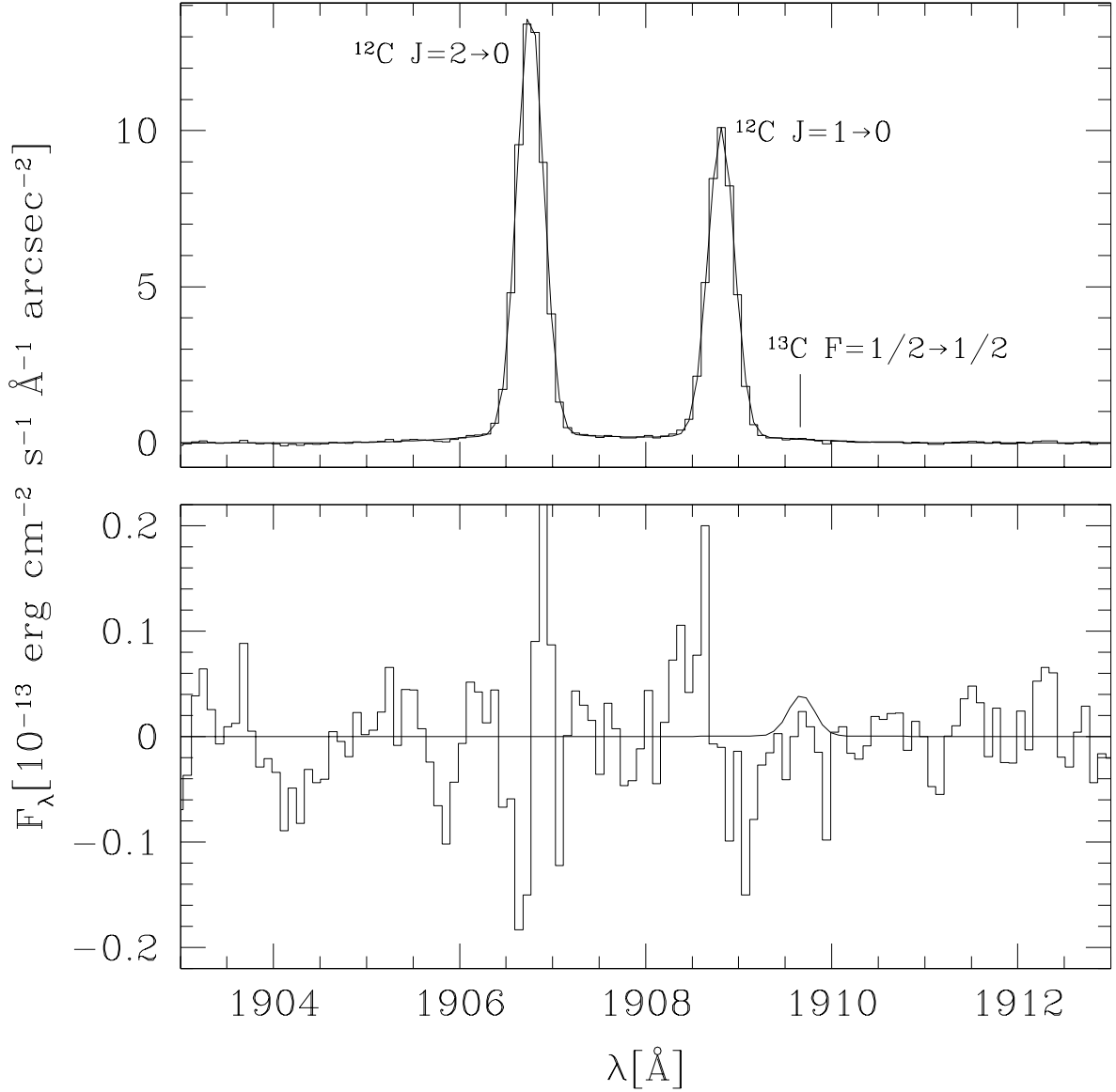


Fig. 1.— HST-STIS spectra of NGC 3242. Upper panel: Observed spectrum (histogram) of the C III] multiplet with the fit superimposed (*solid line*). Lower panel: fit residuals; the *dotted line* represents a ^{13}C line at 1909.6 \AA with a flux ratio of 0.003 relative to the 1906.7 \AA line. The ^{13}C line is not detected, thus setting the value of the firm upper limit $^{12}\text{C}/^{13}\text{C} > 38$.

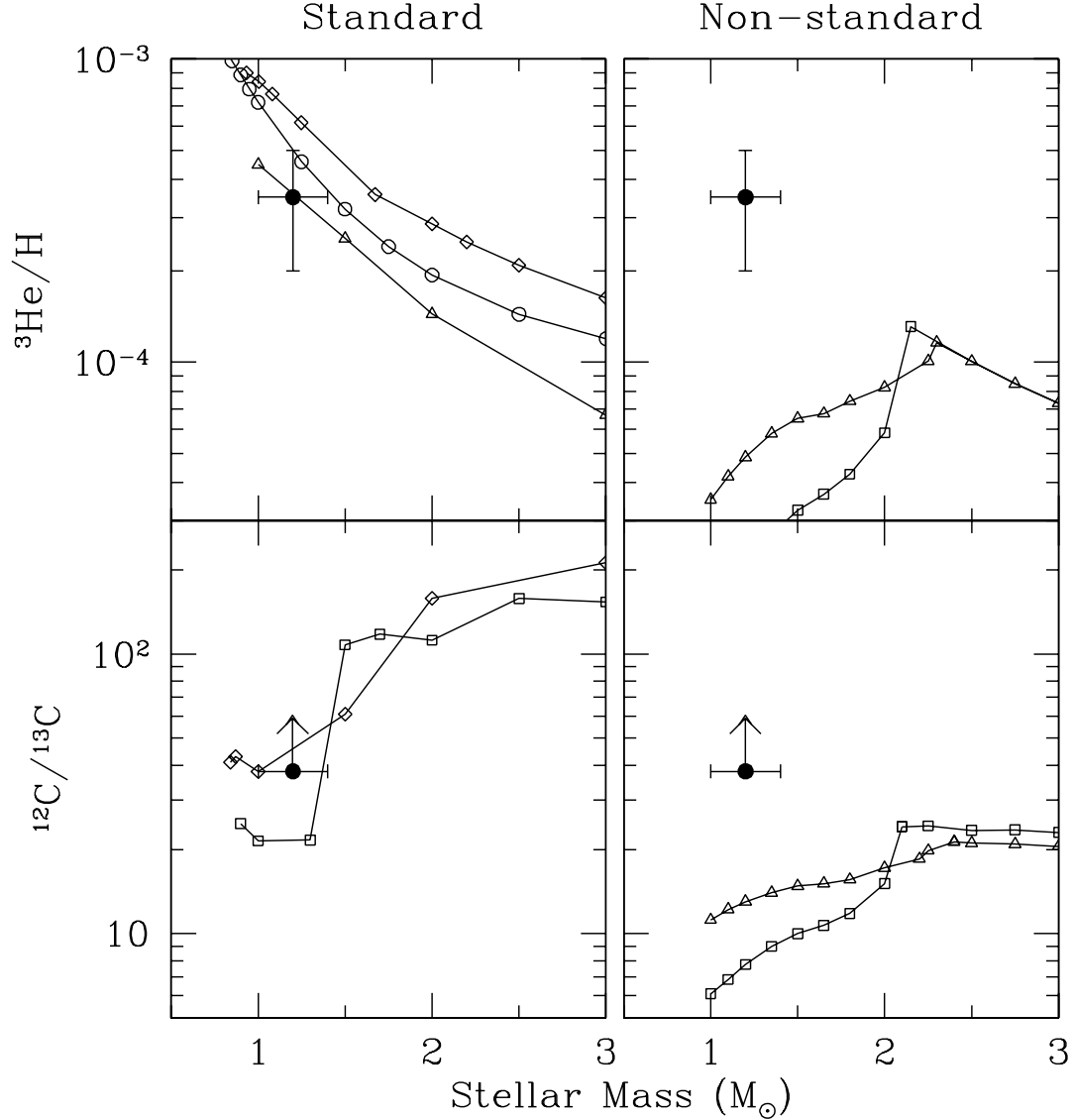


Fig. 2.— Elemental abundances vs. progenitor mass for standard (*left panels*) and non-standard (*right panels*) stellar evolution models. The observed ${}^3\text{He}/\text{H}$ abundance of NGC 3242 (Balsler et al. 1999b) and the lower limit on ${}^{12}\text{C}/{}^{13}\text{C}$ found in this work are indicated by the *filled dots*. The mass estimate of NGC 3242 and associated uncertainty are from Galli et al. (1997). *Standard models*: for ${}^3\text{He}$ the symbols show the models computed by Marigo (2001) (*diamonds*), Weiss et al. (1996) (*triangles*), and Dearborn et al. (1996) (*circles*); for the ${}^{12}\text{C}/{}^{13}\text{C}$ ratio the symbols show the models of van den Hoeck & Groenewegen (1997) (*squares*) and Marigo (2001) (*diamonds*) for the ejecta of stars at the tip of the AGB phase. All models are for solar metallicity. *Non-standard models*: the symbols show the results of Sackmann & Boothroyd (1999) for ${}^3\text{He}$ and Boothroyd & Sackmann (1999) for ${}^{12}\text{C}/{}^{13}\text{C}$: $Z = 0.02$ (*triangles*) and $Z = 0.007$ (*squares*) at the end of the RGB phase.

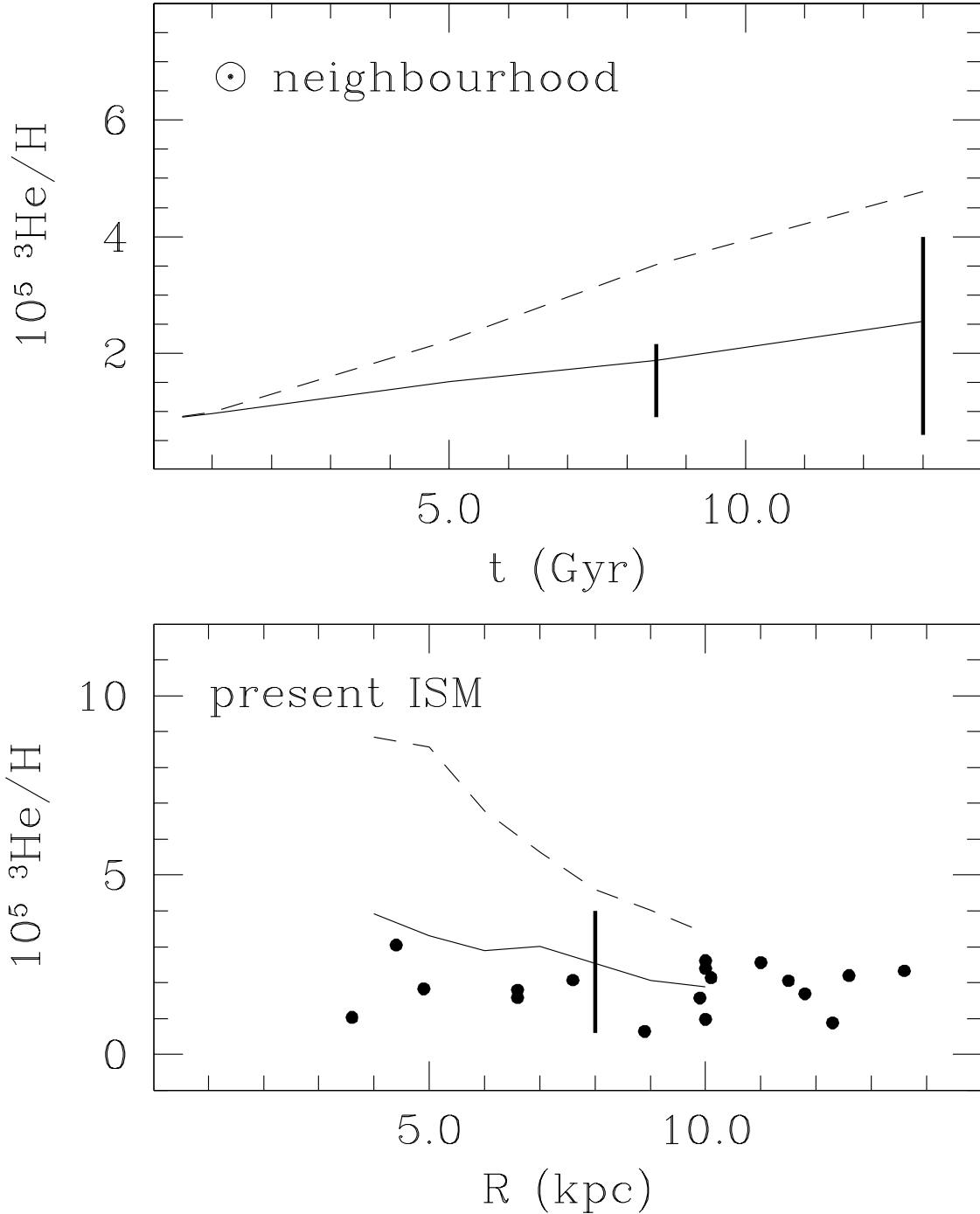


Fig. 3.— Top panel: Galactic chemical evolution of ^3He in the solar neighborhood assuming $(^3\text{He}/\text{H})_0 = 0.9 \times 10^{-5}$ (Palla et al. 2000; Tosi 2001). The *dashed* curve is for a model with standard yields for all stars, while the solid curve corresponds to the same model but adopting the extra-mixing yields by Sackmann & Boothroyd (1999) in 90% of low-mass stars. The vertical bars show the 2σ $^3\text{He}/\text{H}$ abundance for the local ISM and the solar system (Geiss & Gloeckler 1998). Bottom panel: Radial distribution of the ^3He abundance at the present epoch. The data points display the values of Galactic HII regions (Bania et al. 2002), while the vertical bar at 8 kpc is the local ISM value as in the top panel. Line symbols as above.